Published in final edited form as:
Free Radic Res. 2012 September ; 46(9): 1115–1122. doi:10.3109/10715762.2012.692785.

Unique Oxidation of Imidazolidine Nitroxides by Potassium Ferricyanide: Strategy for Designing Paramagnetic Probes with Enhanced Sensitivity to Oxidative Stress

Andrey A. Bobko[†], **Olga V. Efimova**[†], **Maxim A. Voinov**[‡], and **Valery V. Khramtsov**[†,*]

[†]Division of Pulmonary, Allergy, Critical Care and Sleep Medicine, Department of Internal Medicine, The Ohio State University, Columbus, OH 43210

[‡]North Carolina State University, Department of Chemistry, Raleigh, NC 27695

Abstract

Potassium ferricyanide, routinely employed for the oxidation of sterically-hindered hydroxylamines to nitroxides, is considered to be chemically inert towards the latter. In the present study we report on an unexpected oxidative fragmentation of the imidazolidine nitroxides containing hydrogen atom in the 4-position of the heterocycle (HIMD) by potassium ferricyanide resulting in the loss of the EPR signal. The mechanistic EPR, spectrophotometric, electrochemical and HPLC-MS studies support the assumption that the HIMD fragmentation is facilitated by the proton abstraction from the 4-position of the oxoammonium cation formed as a result of the initial one-electron HIMD oxidation. Increase in steric hindrance around the radical fragment by introducing ethyl substituents decreased the rate of ascorbate-induced HIMD reduction by more than 20 times but did not affect the rate of ferricyanide-induced HIMD oxidation. This preferential sensitivity of HIMDs to oxidative processes has been used to detect peroxyl radicals in the presence of high concentration of the reducing agent, ascorbate. HIMD-based EPR probes capable to discriminate oxidative and reductive processes might find application in biomedicine and related fields for monitoring the oxidative stress and reactive radical species in biological systems.

Keywords

nitroxide; sterically-hindered hydroxylamine; oxoammonium cation; electron paramagnetic resonance; redox probes; peroxyl radicals

Introduction

Nitroxides are broadly used in biology and medicine as metabolically responsive contrast-enhancing agents for magnetic resonance imaging (MRI)[1–4], spin labels and probes for EPR studies[5–9], superoxide dismutase (SOD)-mimics[10, 11], antioxidants[12–14] and redox-sensitive dual fluorophore-nitroxide probes [15, 16]. These applications, in part, are based on the knowledge of the redox chemistry of the nitroxides (for reviews see[6, 10, 17, 18]). In biologically relevant systems EPR-detectable nitroxide species can be partially converted into a hydroxylamine - an EPR-silent product of one-electron reduction [17]. The latter form is routinely identified by its stoichiometric re-oxidation to the EPR-detectable parent nitroxide using potassium ferricyanide (PF). PF is a mild one-electron oxidizing agent (E0=0.37 V [19]) and is considered to be chemically inactive towards nitroxide group[6]. This work

Corresponding Author, Valery V. Khramtsov, .201 HLRI, 473 W 12th Ave, Columbus, OH 43210; valery.khramtsov@osumc.edu.

describes our recent observation of unexpected irreversible transformation of the imidazolidine nitroxides containing hydrogen atom in the 4-position of the heterocycle by PF to diamagnetic products. On one hand, this finding makes one aware of the special precautions that should be taken while using ferricyanide for quantification of imidazolidine nitroxides. On the other hand, and more importantly, this observation provides a rational basis for the design of paramagnetic probes with enhanced sensitivity to oxidative processes in biological systems.

Materials and Methods

Reagents

Potassium ferricyanide, $K_3Fe(CN)_6$, potassium ferrocyanide, $K_4Fe(CN)_6 \cdot 3H_2O$, sodium phosphate dibasic, Na_2HPO_4, sodium phosphate monobasic, NaH_2PO_4, were purchased from Fisher Scientific. Diethylene triamine pentaacetic acid (DTPA) was purchased from Acros Organics. 2,2,6,6-tetramethylpiperidine 1-oxyl (TEMPO), 3-carboxy-2,2,5,5-tetramethyl-1-pyrrolidine-1-oxyl (CP), 3-carbamoyl-2,2,5,5-tetramethyl-1-pyrrolidineoxy (CMP) and 2,2,5,5-tetramethyl-3-carbamido-3-pyrroline-1-oxyl (CTPO) were purchased from Sigma-Aldrich. The imidazolidine nitroxides, 2,2,3,4,5,5-hexamethylperhydroimidazol-1-yloxy (HIMD1)[20], 3,4-dimethyl-2,2,5,5-tetraethylperhydroimidazol-1-yloxy (HIMD2)[21] and 2,2,3,4,4,5,5-heptamethylperhydroimidazol-1-yloxy (IMD3) [22] were synthesized as described previously. Imidazoline nitroxide, 2,2,4,5,5-pentamethyl-2,5-dihydro-1H-imidazol-1-yloxy (IM1) was synthesized as described in reference[20]. 2-(4-carboxyphenyl)-4,4,5,5-tetramethylimidazoline-1-oxyl-3-oxide potassium salt (cPTIO) was purchased from Cayman Chemicals. 2,2'-azobis[2-(2-imidazolin-2-yl) propane] dihydrochloride (AIPH) was purchased from Waco Pure Chemical Industries, Ltd. Chemical structures of the nitroxides used in this study are shown in Schemes 1 and 2.

All solutions were prepared in 50 mM Na-phosphate buffer (pH=7.4) containing 0.5 mM DTPA, unless otherwise stated. Water was purified using Milli-Q purification system. Hydroxylamine solutions (0.1 mM) were obtained by the reduction of corresponding nitroxides by excess of ascorbic acid. Re-oxidation of the hydroxylamines back to the parent nitroxides was performed by addition of excess of PF.

EPR measurements

EPR spectra were acquired at room temperature with an EMX X-band EPR spectrometer (Bruker). Solution samples were placed into 50-μl capillary tubes.

UV-vis studies

UV-vis studies were carried out at room temperature using Beckman-Coulter DU800 spectrophotometer.

Cyclic voltammetry studies

Cyclic voltammetry was performed on a potentiostat and computer-controlled electroanalytical system VersaSTAT3. The measurements were carried out in a 10 mL cell equipped with a glassy carbon working electrode (7.07 mm^2), a platinum-wire auxiliary electrode, and Ag/AgCl reference electrode in acetonitrile containing 0.1 M tetrabutylammonium perchlorate and a nitroxide at concentrations from 1.0 to 1.5 mM.

Mass spectrometry studies

To prevent the reaction mixtures from acidification observed during the reaction of HIMD1 and PF, the HPLC-MS studies were carried out in 50 mM Na-phosphate buffer, pH=7.4. HPLC-MS measurements were carried out using Ultimate 3000 DIONEX HPLC equipped with Q-

TOF-2 mass spectrometer. HPLC conditions were: column, Vydac C18, 300 Å 5 μm, 1×250 mm; gradient conditions: a linear gradient of acetonitrile-0.1% formic acid (5 to 90% over 15 min and a flow rate of 25 μL/min) against 0.1% aqueous formic acid. HPLC was followed by electrospray ionization mass spectrometry (ESI-MS) detection in positive ion mode.

Results

The main product of nitroxide metabolism in biological systems, hydroxylamine, is routinely identified by its re-oxidation to the EPR-detectable parent nitroxide using PF, which is considered to be chemically inactive towards nitroxide[6]. Accordingly, our re-examination showed stoichiometric recovery of representative nitroxides of piperidine, pyrrolidine, pyrroline, and 3-imidazoline series (Scheme 1), as well as imidazolidine nitroxide IMD3 (Scheme 2), from the corresponding hydroxylamines after re-oxidation with PF. The integral EPR spectral intensities of these nitroxides were not affected by the presence of excess of PF (1–10 mM) for at least several hours.

Surprisingly, imidazolidine nitroxides with hydrogen atom at C4 position of the heterocycle, HIMD1 and HIMD2 (Scheme 2), revealed a complete loss of the EPR signal in the presence of PF (Fig. 1). Complementary UV-vis studies showed a concomitant decay of PF absorption as a result of its reduction to potassium ferrocyanide. Comparison of the HIMD1 and PF decays measured by EPR and UV-vis absorption, respectively, showed the [HIMD1]:[PF] stoichiometry being equal to 1:1 for the initial parts of the kinetic curves (Fig. 1). Reduction of $K_3Fe(CN)_6$ was found to be reversible as confirmed by the re-oxidation of ferrocyanide anion back to PF by PbO_2 (data not shown). In contrast, the oxidation of the HIMD radicals resulted in an irreversible loss of the EPR signals. The rates of HIMD1 and HIMD2 oxidation by PF were found to be linearly dependent on $K_3Fe(CN)_6$ concentration allowing for calculation of the corresponding bimolecular rate constants (Fig. 2).

Previously we reported that increase in steric hindrance around the N−O$^\bullet$ group in the HIMD2 radical decreases the rate of its reduction by ascorbate by more than 20 times compared to that of HIMD1[23]. However, only small difference in the rate constants was observed for the ferricyanide-induced oxidation of the HIMD1 and HIMD2.

Comparative electrochemical study also suggested a more facile oxidation of HIMD radicals relative to the nitroxides of piperidine (TEMPO), imidazoline (IM1), and imidazolidine (IMD3) series. Thus, cyclic voltammogram for acetonitrile solution of TEMPO clearly showed a one-electron reversible oxidation, whereas that of IM1 and IMD3 showed a quasi-reversible character (see Fig. 3), which is in an agreement with the previously reported reversible oxidation of the N−O$^\bullet$ group of piperidine and imidazoline nitroxides to oxoammonium cation [24][25]. On the contrary, cyclic voltammograms of HIMD1 and HIMD2 showed an irreversible oxidation pattern (Fig. 3D), most likely due to a cleavage of the C5−N1 bond in the oxoammonium cation promoted by a proton abstraction from the 4-position of the heterocycle. Note that the redox potential of ferri-ferrocyanide couple in acetonitrile is E^0 = 0.37 V[19] and oxidation potentials of HIMDs, $E^0 \approx 0.60 \div 0.67$ V (Table 1). Therefore, thermodynamically oxidation of HIMD1 and HIMD2 by ferricyanide anion is only slightly unfavorable and can be driven kinetically by the irreversible character of the reaction.

To further investigate the mechanism of the HIMD oxidation the HPLC-MS studies of the reaction of HIMD1 with PF were performed. HPLC conditions were optimized for separation of anions of phosphate, ferricyanide and ferrocyanide from organic compounds, HIMD1 and products of its reaction (Fig. 4A). Typically, ESI-MS spectra of the nitroxides are characterized by the peaks of the following ions: (i) oxoammoinium cation $[M]^+$; (ii) protonated radical cation $[M+H]^{+\bullet}$ and (iii) protonated hydroxylamine cation $[M+2H]^+$. The relative abundance

of these ions strongly depends on the structure of the radical, the solvent, and the ionization conditions[26]. The HPLC retention time for HIMD1 was found to be about 7.5 min and the mass spectrum of HIMD1 was characterized by ions with m/z = 172 and 173 (Figs. 3, traces c), corresponding to $[M+H]^+$● **8** and $[M+2H]^+$ **9** ions, respectively (Scheme 3). The peak of the oxoammonium cation **4** with m/z=171 was not observed in the mass spectrum, most likely because of its fast decomposition. One-hour room temperature incubation of HIMD1 with half equivalent of PF resulted in decrease of intensity of HPLC signal of the former and appearance of additional HPLC signal with retention time of about 8 min (Figs. 4A and 4B, traces d). This unresolved HPLC peak is characterized by mass spectrum with m/z = 171 and 169 (Figs. 4B and 4C, traces d). Note that the peak with m/z = 171 could be assigned both to the oxoammonium cation 4 and enamine cation 10 (Scheme 3).

A plausible scheme of the HIMD1 fragmentation caused by the reaction with PF is shown in Scheme 3. The initial step of the reaction is supposed to be a one-electron oxidation of the N−O• group to oxoammonium cation **4**. A reversible character of this step was supported by a significant decrease of the rate of PF-induced decay of HIMDs in the presence of excess of potassium ferrocyanide (data not shown). Similar to the decomposition of oxoammonium cation in a series of piperidine[27–29] and pyrrolidine[30] nitroxides, heterolytic cleavage of the C5−N1 bond of **4** is facilitated by the proton abstraction from C4, thus lowering the activation energy for the reaction resulting in the formation of stable enamine **6**. Electrospray ionization of this compound produces an $[M+H]^+$ ion **10** that appears in the mass spectrum at m/z=171. Room temperature incubation of HIMD1 with 20-fold excess of PF for 10 hours resulted in complete disappearance of HPLC peak of HIMD1 at 7.5 min and increase in the intensity of HPLC peak with 8 min retention time. Based on the mass of the ion corresponding to this peak ($[M]^+$, m/z=169, Figs. 4B and 4C, traces e), the peak was assigned the structure of the eniminium cation **7**. The latter was most likely formed through a mechanism similar to that proposed earlier for oxidation of tertiary amines by PF[31].

Irreversible degradation of HIMD into EPR silent products caused by an oxidizing reagent presents a pathway to design redox sensitive EPR probes with preferential sensitivity to oxidative vs. reductive processes. Indeed, although the steric hindrance around the N−O• group, such as in HIMD2, significantly decreases HIMDs reactivity towards reducing agents[23], it may not affect the reactivity of HIMDs towards the oxidizing species, as it was observed for PF (see Fig. 2 and Table 1). To illustrate this statement, we measured the rates of HIMD1 and HIMD2 reactions with peroxyl radicals. Thermal decomposition of 2,2'-azobis[2-(2-imidazolin-2-yl) propane] dihydrochloride (AIPH) in air saturated solutions was used as a source of peroxyl radicals[32, 33]. In these conditions AIPH decays with the formation of two alkyl radicals, which, in turn, react with dissolved oxygen with a diffusion-controlled rate constant[34] of ~$10^9 M^{-1}s^{-1}$, generating peroxyl radicals, ROO•[32]. The EPR spectra of the nitroxides of the pyrroline series, CP and CMP, widely used as redox sensitive probes[4, 35–38], and imidazoline nitroxide IM1, were found to be unchanged upon incubation with AIPH (data not shown). On contrary, the decay rates for the HIMDs in peroxyl radical-generating system (Fig. 5, empty squares) were close to the rate of ROO• generation by AIPH, thus supporting highly efficient, if not complete, scavenging of the ROO• by HIMDs. In spite of the increase in steric hindrance around the N–O• fragment of HIMD2, HIMD1 showed a slightly slower decay of the EPR signal in the presence of AIPH (cf. empty squares in Figs. 5A and 5B). Still, the initial rate of HIMD1 reduction by ascorbate was in about 20 times higher compared to that of HIMD2 (cf. empty circles in Figs. 5A and 5B). As a consequence, in the presence of both agents the HIMD1 signal decay was hardly distinguishable from that upon the reduction (cf. open and filled circles in Fig. 5A), while for HIMD2, the contribution of the oxidation in the signal decay was predominant (cf. squares and filled circles, Fig. 5B). Partial inhibition of the AIPH-induced HIMD2 decay by ascorbate (cf. squares and filled circles in Fig. 5B) is in agreement with competitive scavenging of peroxyl radicals by ascorbate (rate

constant about 2×10^6 $M^{-1}s^{-1}$ [39]). The rate constant of the reaction of HIMD2 with $ROO^\bullet$ estimated from inhibition of HIMD2 decay by ascorbate was found to be $\geq 5\times10^8$ $M^{-1}s^{-1}$, which is among the highest rate constants reported for the scavenging of peroxyl radicals. The high rate constant of the HIMDs oxidation by $ROO^\bullet$ is not surprising taking into account a much higher oxidation potential of peroxyl radicals (E^0 ranging from 0.77 to 1.44 V[40] vs. E^0 =0.37 V[19] for ferricyanide).

Discussion

The main product of nitroxide metabolism in biological systems, hydroxylamine, is routinely identified by its re-oxidation to the EPR-measured parent nitroxide using PF. This procedure allows for quantification of hydroxylamines by EPR techniques and is based on the assumptions that i) the equilibrium of the oxidation reaction is strongly shifted toward the nitroxide, and ii) the nitroxide is stable in the presence of PF. Here we demonstrate that the latter statement, while being valid for the most of the nitroxide series, is not applied to the nitroxides of the imidazolidine series containing hydrogen atom in the 4-position of the heterocycle (HIMDs). As we discovered, the HIMD nitroxides easily undergo oxidative fragmentation in the presence of PF. This fragmentation turns the HIMD nitroxides into EPR silent products. Mechanistic studies support the assumption that the HIMD fragmentation is facilitated by the proton abstraction from the 4-position of the oxoammonium cation resulted from initial one-electron oxidation of HIMD by PF (Scheme 3). Increase in steric hindrance around the $N-O^\bullet$ fragment does not affect significantly the rate of the HIMD reaction with the oxidizing species (see Figs. 2, 5 and Table 1). This observation is in line with our previous finding that the rates of the oxidation of the hydroxylamines – derivatives of HIMD1 and HIMD2 – with ascorbyl radical are essentially the same [21]. Thus, the oxidation rates of the HIMDs and their hydroxylamine derivatives seem do not depend significantly on the steric hindrance around the $N-O^\bullet$ fragment. But, as we know, the rate of the nitroxide reduction can be decreased by an order of magnitude by increasing the steric hindrance around the $N-O^\bullet$ fragment[23, 41, 42]. This discrepancy seems to stem from the fundamental difference in the mechanisms of the oxidation and reduction; the oxidation of the nitroxide to the oxoammonium cation requires only electron transfer, while the reduction requires both electron and proton transfer to take place[6]. The latter process involves reorganization of the proton donor (solvent) molecules in the vicinity of the nitroxide group, e.g. hydrogen bond formation[6], and apparently is more demanding to the steric conditions around the $N-O^\bullet$ fragment.

The rates of the nitroxide decay measured by EPR[35, 43, 44] and MRI[3, 36] have been shown to provide information on tissue redox status *in vivo*. Typically, the nitroxide decay in biological systems is attributed to the tissue reducing capacity[4, 35]. Nevertheless, serious efforts have been undertaken to extract from the rate of the nitroxide decay the information on oxidative processes, in particular that related to generation of reactive radical species (RRS) in various pathological conditions[37, 45, 46]. Currently, there is a consensus that *in vivo* nitroxide decay reflects the overall tissue redox status, while discrimination between contributions from reducing and oxidizing species requires independent experiments, e.g. using exogenous antioxidants or radical scavengers.

The observed facile irreversible oxidation of HIMDs by potassium ferricyanide resulting in the loss of the EPR signal opens a way to designing EPR probes with enhanced sensitivity to RRS and related oxidative processes and discriminating between oxidative and reductive processes in biological systems by means of EPR spectroscopy. The oxidation potential of HIMDs of about $E^0 \approx 0.6$ V (Table 1) is significantly lower than that of the most biologically relevant RRS such as superoxide, hydroxyl, peroxyl or lipid-derived radicals, which makes the reaction of HIMDs with RRS thermodynamically highly feasible. Molecular design of such a probe can be accomplished through the protection of the $N-O^\bullet$ fragment of the nitroxide

towards reduction by flanking it with bulky substituents similar to that in HIMD2. A viability of this approach was demonstrated by monitoring the peroxyl radicals formation in the presence of a high concentration of ascorbic acid as a reducing agent (Fig. 5). Preferential sensitivity of the HIMDs with sterically hindered N−O• group towards oxidation is of particular interest for non-invasive *in vivo* EPR applications in biological systems where the role of RRS in oxidative metabolism and redox signaling is widely discussed[3, 35, 47–50]. We speculate that simultaneous use of two HIMD derivatives, the one containing more sterically protected ^{14}N−O• group and the other one, containing less sterically protected ^{15}N−O• group, would allow for extraction of a real-time information on both reducing and oxidizing capacities of the microenvironment[51]. In order to optimize the structure of the probe and to develop reliable protocols for monitoring the oxidative processes in biological systems with EPR, further kinetics studies of the reactions of the HIMDs with different types of RRS are required. These results will be described in details in a separate publication.

Supplementary Material

Refer to Web version on PubMed Central for supplementary material.

Acknowledgments

The authors thank Dr. I.A. Kirilyuk for the providing of HIMD2 compound, Mr. S.V. Semenov for the assistance with the initial EPR experiments and Dr. F. Villamena for the assistance with the cyclic voltammetric measurements. This work was partially supported by NIH grants HL089036 and EB014542-01A1. M.A.V. thanks the U.S. Department of Energy's Office of Basic Energy Sciences for financial support (Grant DE-FG02-02ER15354).

ABBREVIATIONS

PF	potassium ferricyanide
IM	imidazoline nitroxide
IMD	imidazolidine nitroxide
HIMD	imidazolidine nitroxide containing hydrogen atom in the 4-position of the heterocycle
RRS	reactive radical species

REFERENCES

1. Gallez B, Bacic G, Goda F, Jiang J, O'Hara JA, Dunn JF, Swartz HM. Use of nitroxides for assessing perfusion, oxygenation, and viability of tissues: in vivo EPR and MRI studies. Magn Reson Med. 1996; 35:97–106. [PubMed: 8771027]
2. Winalski CS, Shortkroff S, Schneider E, Yoshioka H, Mulkern RV, Rosen GM. Targeted dendrimer-based contrast agents for articular cartilage assessment by MR imaging. Osteoarthritis Cartilage. 2008; 16:815–822. [PubMed: 18226558]
3. Matsumoto K, Hyodo F, Matsumoto A, Koretsky AP, Sowers AL, Mitchell JB, Krishna MC. High-resolution mapping of tumor redox status by magnetic resonance imaging using nitroxides as redox-sensitive contrast agents. Clin Cancer Res. 2006; 12:2455–2462. [PubMed: 16638852]
4. Hyodo F, Matsumoto K, Matsumoto A, Mitchell JB, Krishna MC. Probing the intracellular redox status of tumors with magnetic resonance imaging and redox-sensitive contrast agents. Cancer Res. 2006; 66:9921–9928. [PubMed: 17047054]
5. Berliner, LJ. The Next Millennium. New York: Plenum Press; 1998. Spin Labeling.
6. Kocherginsky, N.; Swartz, HM. Nitroxide spin labels. Reactions in biology and chemistry. CRC Press; 1995.

7. Khan, N.; Khramtsov, VV.; Swartz, H. M. Methods for Tissue pO2, Redox pH Glutathione Measurements by EPR Spectroscopy. In: Das, D., editor. Methods in Redox Signaling. New Rochelle, NY: Mary Ann Liebert, Inc; 2009. p. 79-87.
8. Khramtsov, VV.; Zweier, JL. Functional in vivo EPR Spectroscopy and Imaging Using Nitroxide and Trityl Radicals. In: Hicks, R., editor. Stable Radicals: Fundamentals and Applied Aspects of Odd-Electron Compounds. New Rochelle, NY: John Wiley & Sons, Ltd; 2010. p. 537-566.
9. Khramtsov, V.; Volodarsky, L. Biological Magnetic Resonance. US: Springer; 2002. Use of Imidazoline Nitroxides in Studies of Chemical Reactions ESR Measurements of the Concentration and Reactivity of Protons, Thiols, and Nitric Oxide; p. 109
10. Soule BP, Hyodo F, Matsumoto K, Simone NL, Cook JA, Krishna MC, Mitchell JB. The chemistry and biology of nitroxide compounds. Free Radic Biol Med. 2007; 42:1632–1650. [PubMed: 17462532]
11. Mitchell, JB.; Krishna, MC.; Samuni, A.; Kuppusamy, P.; Hann, SM.; Russo, A. Clinical uses of nitroxides as superoxide-dismutase mimics. In: Rhodes, CJ., editor. Toxicology of the human environment: the critical role of free radicals. London, New York: Taylor & Francis Inc; 2000. p. 113-138.
12. Krishna MC, Samuni A. Nitroxides as antioxidants. Methods Enzymol. 1994; 234:580–589. [PubMed: 7808334]
13. Damiani E, Belaid C, Carloni P, Greci L. Comparison of antioxidant activity between aromatic indolinonic nitroxides and natural and synthetic antioxidants. Free Radic Res. 2003; 37:731–741. [PubMed: 12911269]
14. Soule BP, Hyodo F, Matsumoto K, Simone NL, Cook JA, Krishna MC, Mitchell JB. Therapeutic and clinical applications of nitroxide compounds. Antioxid Redox Signal. 2007; 9:1731–1743. [PubMed: 17665971]
15. Blough NV, Simpson DJ. Chemically mediated fluorescence yield switching in nitroxide–fluorophore adducts: optical sensors of radical/redox reactions. J Am Chem Soc. 1988; 110:1915–1917.
16. Morrow BJ, Keddie DJ, Gueven N, Lavin MF, Bottle SE. A novel profluorescent nitroxide as a sensitive probe for the cellular redox environment. Free Radic Biol Med. 2010; 49:67–76. [PubMed: 20350596]
17. Swartz, HM.; Timmins, GS. The metabolism of nitroxides in cells and tissues. In: Rhodes, CJ., editor. Toxicology of the human environment: the critical role of free radicals. London, New York: Taylor & Francis Inc; 2000. p. 91-111.
18. Wilcox CS, Pearlman A. Chemistry and antihypertensive effects of tempol and other nitroxides. Pharmacol Rev. 2008; 60:418–469. [PubMed: 19112152]
19. Rao SP, Singh SR, Bandakavi SR. Formal redox potentials of ferricyanide-ferrocyanide couple in certain nonaqueous water mixtures. Proc. Nat. Acad. Sci. India A. 1978; 44:333–335.
20. Volodarsky, LB.; Grigor'ev, IA.; Sagdeev, RZ. Stable Imidazoline Nitroxides. In: Berliner, LJ.; Reuben, J., editors. Biological Magnetic Resonance. New York: Plenum Press; 1980. p. 169-242.
21. Bobko AA, Kirilyuk IA, Grigor'ev IA, Zweier JL, Khramtsov VV. Reversible reduction of nitroxides to hydroxylamines: roles for ascorbate and glutathione. Free Radic Biol Med. 2007; 42:404–412. [PubMed: 17210453]
22. Volodarsky, LB.; Reznikov, VA.; Grigor'ev, IA. Chemical properties of heterocyclic nitroxides. In: Volodarsky, LB., editor. Imidazoline Nitroxides. Boca Raton, Fl: CRC Press; 1988. p. 29-76.
23. Kirilyuk IA, Bobko AA, Grigor'ev IA, Khramtsov VV. Synthesis of the tetraethyl substituted pH-sensitive nitroxides of imidazole series with enhanced stability towards reduction. Org Biomol Chem. 2004; 2:1025–1030. [PubMed: 15034626]
24. Blinco JP, Hodgson JL, Morrow BJ, Walker JR, Will GD, Coote ML, Bottle SE. Experimental and theoretical studies of the redox potentials of cyclic nitroxides. J Org Chem. 2008; 73:6763–6771. [PubMed: 18683980]
25. Shchukin, GI.; Grigor'ev, IA. Oxidation-reduction properties of nitroxides. In: Volodarsky, LB., editor. Imidazoline Nitroxides. Boca Raton, FL: CRC Press; 1988. p. 171-214.
26. Marshall DL, Christian ML, Gryn'ova G, Coote ML, Barker PJ, Blanksby SJ. Oxidation of 4-substituted TEMPO derivatives reveals modifications at the 1- and 4-positions. Org Biomol Chem. 2011; 9:4936–4947. [PubMed: 21597620]

27. Goldstein S, Samuni A, Russo A. Reaction of cyclic nitroxides with nitrogen dioxide: the intermediacy of the oxoammonium cations. J Am Chem Soc. 2003; 125:8364–8370. [PubMed: 12837108]
28. Nilsen A, Braslau R. Nitroxide decomposition: Implications toward nitroxide design for applications in living free-radical polymerization. Journal of Polymer Science Part A: Polymer Chemistry. 2006; 44:697–717.
29. Ma Y, Loyns C, Price P, Chechik V. Thermal decay of TEMPO in acidic media via an N-oxoammonium salt intermediate. Org Biomol Chem. 9:5573–5578. [PubMed: 21709900]
30. Jia M, Tang Y, Lam YF, Green SA, Blough NV. Prefluorescent nitroxide probe for the highly sensitive determination of peroxyl and other radical oxidants. Anal Chem. 2009; 81:8033–8040. [PubMed: 19788316]
31. Smith JRL, Mead LAV. Amine oxidation. Part VII. The effect of structure on the reactivity of alkyl tertiary amines towards alkaline potassium hexacyanoferrate(III). Journal of the Chemical Society, Perkin Transactions. 1973; 2:206.
32. Niki E. Free radical initiators as source of water- or lipid-soluble peroxyl radicals. Methods Enzymol. 1990; 186:100–108. [PubMed: 2233287]
33. Yoshida Y, Itoh N, Saito Y, Hayakawa M, Niki E. Application of Water-Soluble Radical Initiator, 2,2вЂІ-Azobis-[2-(2-imidazolin-2-yl)propane] Dihydrochloride, to a Study of Oxidative Stress. Free Radical Research. 2004; 38:375–384.
34. Neta P, Huie RP. Rate constants for reaction of peroxyl radicals in fluid solutions. J.Phys.Chem.Ref.Data. 1990; 19:413–513.
35. Kuppusamy P, Li H, Ilangovan G, Cardounel AJ, Zweier JL, Yamada K, Krishna MC, Mitchell JB. Noninvasive imaging of tumor redox status and its modification by tissue glutathione levels. Cancer Res. 2002; 62:307–312. [PubMed: 11782393]
36. Hyodo F, Chuang KH, Goloshevsky AG, Sulima A, Griffiths GL, Mitchell JB, Koretsky AP, Krishna MC. Brain redox imaging using blood-brain barrier-permeable nitroxide MRI contrast agent. J Cereb Blood Flow Metab. 2008; 28:1165–1174. [PubMed: 18270519]
37. Utsumi H, Yamada K. In vivo electron spin resonance-computed tomography/nitroxyl probe technique for non-invasive analysis of oxidative injuries. Arch Biochem Biophys. 2003; 416:1–8. [PubMed: 12859975]
38. Phumala N, Ide T, Utsumi H. Noninvasive evaluation of in vivo free radical reactions catalyzed by iron using in vivo ESR spectroscopy. Free Radic Biol Med. 1999; 26:1209–1217. [PubMed: 10381192]
39. McCay PB. Vitamin E: interactions with free radicals and ascorbate. Annu Rev Nutr. 1985; 5:323–340. [PubMed: 2992548]
40. Buettner GR. The pecking order of free radicals and antioxidants: lipid peroxidation, alphatocopherol, and ascorbate. Arch Biochem Biophys. 1993; 300:535–543. [PubMed: 8434935]
41. Marx L, Chiarelli R, Guiberteau T, Rassat A. A comparative study of the reduction by ascorbate of 1,1,3,3-tetraethylisoindolin-2-yloxyl and of 1,1,3,3-tetramethylisoindolin-2-yloxyl. J. Chem. Soc., Perkin Trans. 2000; 1:1181–1182.
42. Kinoshita Y, Yamada KI, Yamasaki T, Mito F, Yamato M, Kosem N, Deguchi H, Shirahama C, Ito Y, Kitagawa K, Okukado N, Sakai K, Utsumi H. In vivo evaluation of novel nitroxyl radicals with reduction stability. Free Radic Biol Med. 2010; 49:1703–1709. [PubMed: 20828609]
43. He G, Kutala VK, Kuppusamy P, Zweier JL. In vivo measurement and mapping of skin redox stress induced by ultraviolet light exposure. Free Radic Biol Med. 2004; 36:665–672. [PubMed: 14980709]
44. Yamada K, Inoue D, Matsumoto S, Utsumi H. In vivo measurement of redox status in streptozotocin-induced diabetic rat using targeted nitroxyl probes. Antioxid Redox Signal. 2004; 6:605–611. [PubMed: 15130287]
45. Kasazaki K, Yasukawa K, Sano H, Utsumi H. Non-invasive analysis of reactive oxygen species generated in NH4OH-induced gastric lesions of rats using a 300 MHz in vivo ESR technique. Free Radic Res. 2003; 37:757–766. [PubMed: 12911272]
46. Takeshita K, Takajo T, Hirata H, Ono M, Utsumi H. In vivo oxygen radical generation in the skin of the protoporphyria model mouse with visible light exposure: an L-band ESR study. J Invest Dermatol. 2004; 122:1463–1470. [PubMed: 15175038]

47. Hyodo F, Yasukawa K, Yamada K, Utsumi H. Spatially resolved time-course studies of free radical reactions with an EPRI/MRI fusion technique. Magn Reson Med. 2006; 56:938–943. [PubMed: 16964613]

48. Yamada K, Yamamiya I, Utsumi H. In vivo detection of free radicals induced by diethylnitrosamine in rat liver tissue. Free Radic Biol Med. 2006; 40:2040–2046. [PubMed: 16716904]

49. Utsumi H, Yasukawa K, Soeda T, Yamada K, Shigemi R, Yao T, Tsuneyoshi M. Noninvasive mapping of reactive oxygen species by in vivo electron spin resonance spectroscopy in indomethacin-induced gastric ulcers in rats. J Pharmacol Exp Ther. 2006; 317:228–235. [PubMed: 16339915]

50. Swartz HM, Khan N, Khramtsov VV. Use of Electron Paramagnetic Resonance Spectroscopy to Evaluate the Redox State In Vivo. Antioxid. Redox Signal. 2007; 9:1757–1771. [PubMed: 17678441]

51. Utsumi H, Yamada K, Ichikawa K, Sakai K, Kinoshita Y, Matsumoto S, Nagai M. Simultaneous molecular imaging of redox reactions monitored by Overhauser-enhanced MRI with 14N- and 15N-labeled nitroxyl radicals. Proc Natl Acad Sci U S A. 2006; 103:1463–1468. [PubMed: 16432234]

52. Krishna MC, Grahame DA, Samuni A, Mitchell JB, Russo A. Oxoammonium cation intermediate in the nitroxide-catalyzed dismutation of superoxide. Proc Natl Acad Sci U S A. 1992; 89:5537–5541. [PubMed: 1319064]

53. Approximation of decomposition rate constant values at 40, 60 °C published in supplier's (Waco Pure Chemical Industries, Ltd.) product information sheet to the room temperature of 22 °C.

54. Barclay LRC, Locke SJ, MacNeil JM, VanKessel J, Burton GW, Ingold KU. Autoxidation of micelles and model membranes. Quantitative kinetic measurements can be made by using either water-soluble or lipid-soluble initiators with water-soluble or lipid-soluble chain-breaking antioxidants. Journal of the American Chemical Society. 1984; 106:2479.

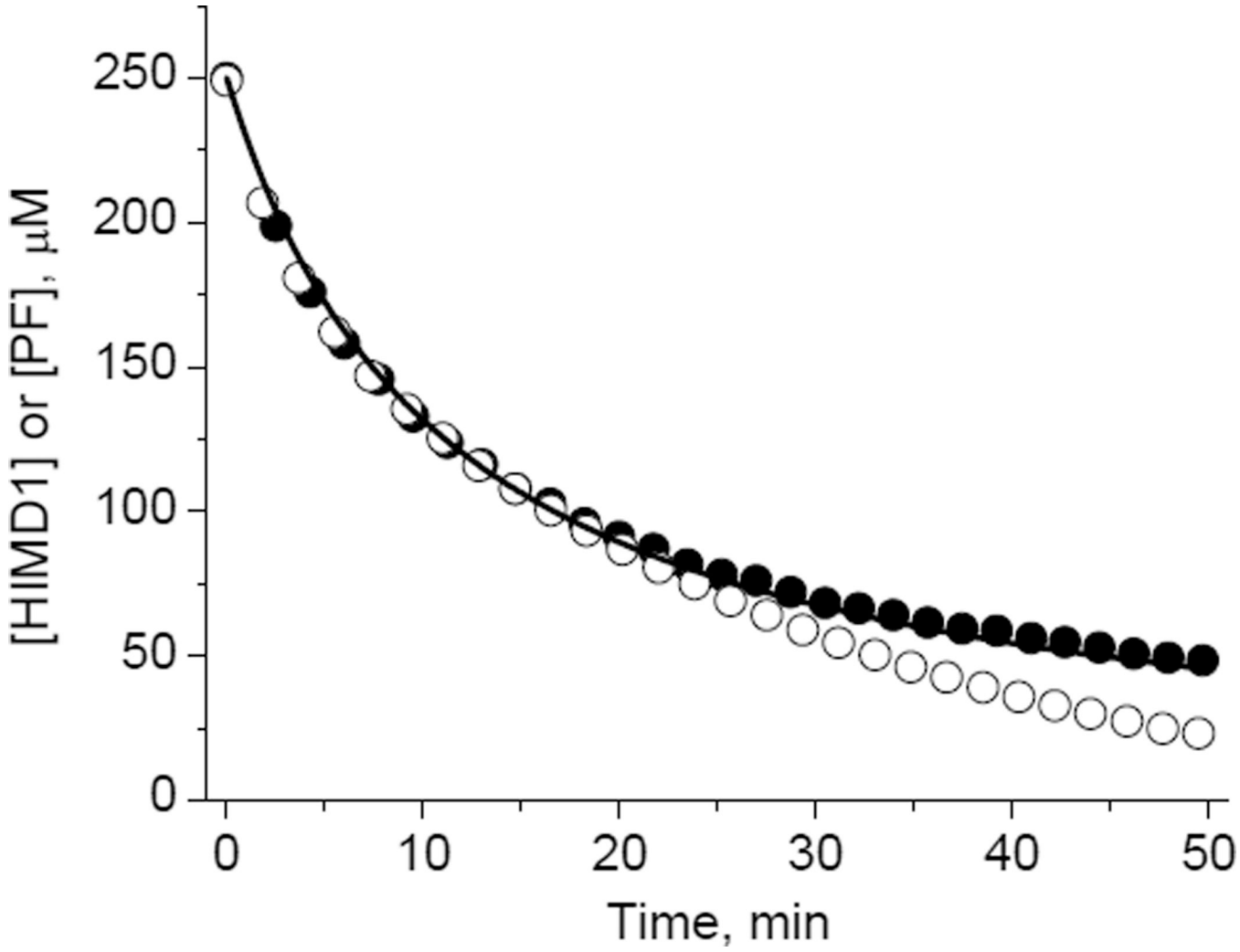

Figure 1.

Kinetics of the decay of HIMD1 nitroxide (●) and PF (○) measured by EPR and UV-vis ($\varepsilon_{420} = 10^3$ $M^{-1}cm^{-1}$), respectively. Initial concentrations of the reagents, C_0, were equal to 250 μM. The solid line is non-linear least-squares fit of the data using equation, $[HMD1]= C_0/(1+k_{ox}\times C_0\times t)$, yielding the bimolecular rate constant of HMD1 oxidation, $k_{ox}=6$ $M^{-1}s^{-1}$. Note that deviation of the measured decays from the stoichiometry [HIMD1]/[PF] = 1:1 is observed only after 20 min of incubation when more than 60% of the reagents are consumed, and might be due to additional PF consumption by the reaction products.

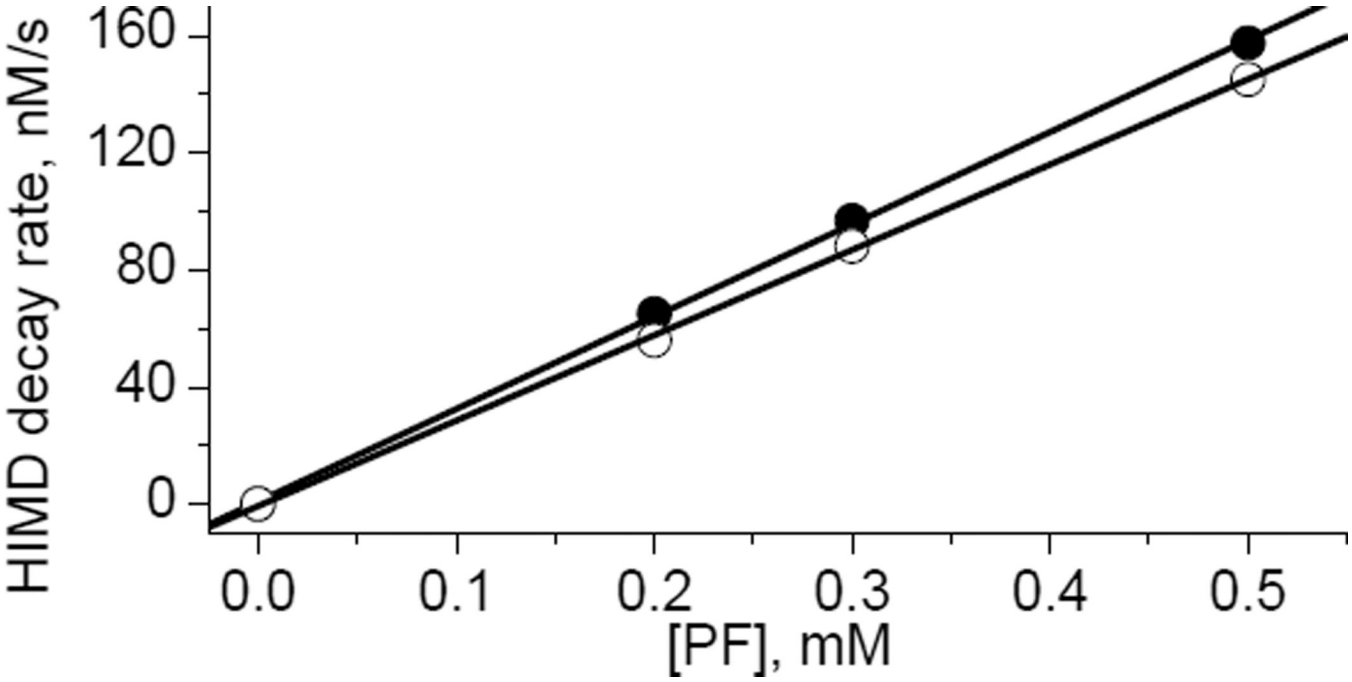

Figure 2.

The dependence of the initial decay rate of HIMD1 (●, $C_0 = 50$ μM) and HIMD2 (○, $C_0 = 50$ μM) on the PF concentration. Solid lines represent linear fit yielding bimolecular rate constant (6.3±0.6) $M^{-1}s^{-1}$ and (5.8±0.6) $M^{-1}s^{-1}$ for the oxidation of HIMD1 and HIMD2 by PF, respectively.

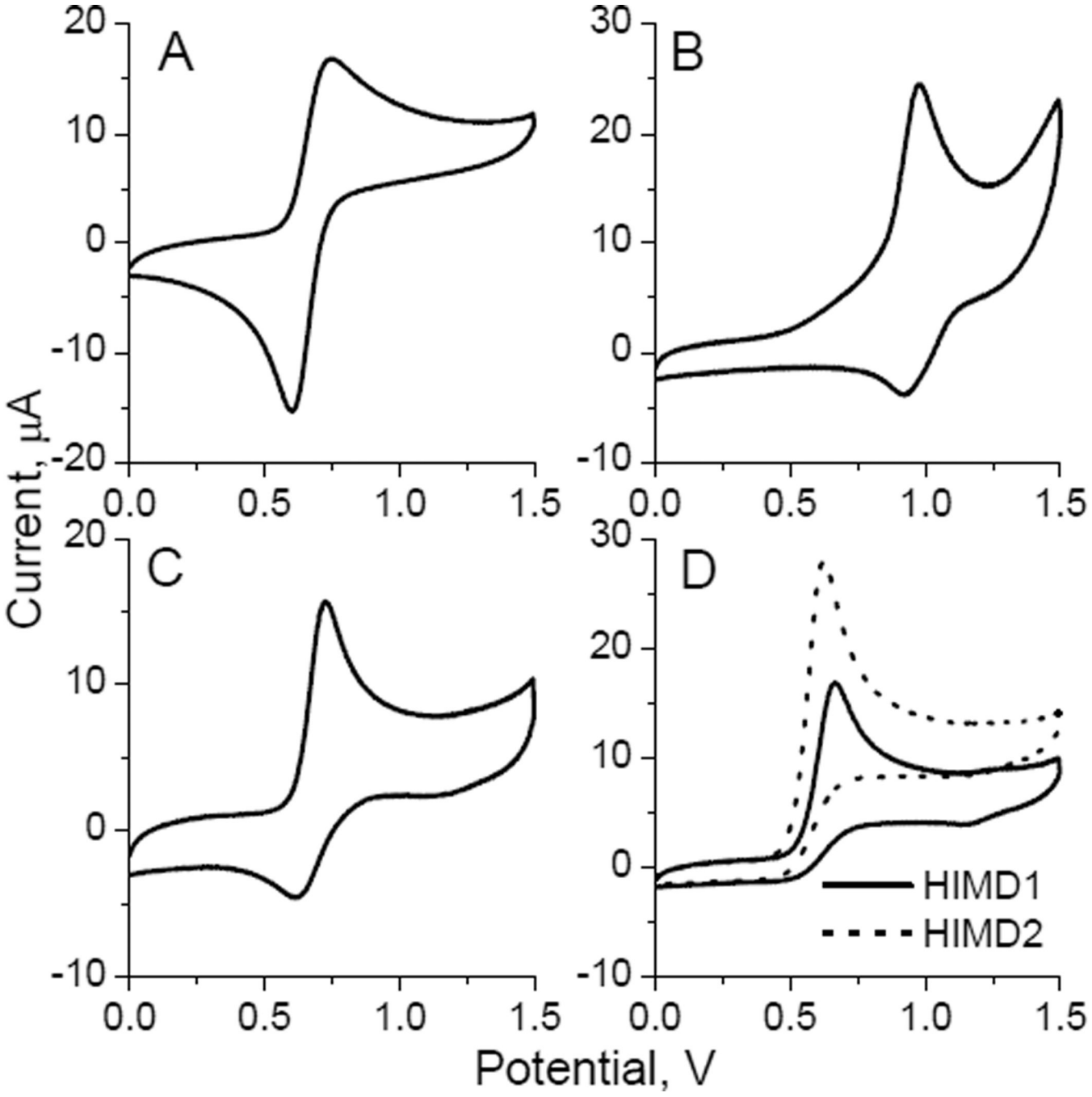

Figure 3.
Cyclic voltammograms of the TEMPO (**A**), IM1 (**B**), IMD3 (**C**), HIMD1 and HIMD2 (**D**) obtained in acetonitrile solution of 0.1 M tetrabutylammonium perchlorate using a glassy carbon and Ag/AgCl electrodes as a working and a reference electrode, respectively. Sweep rate is 0.1 V/s.

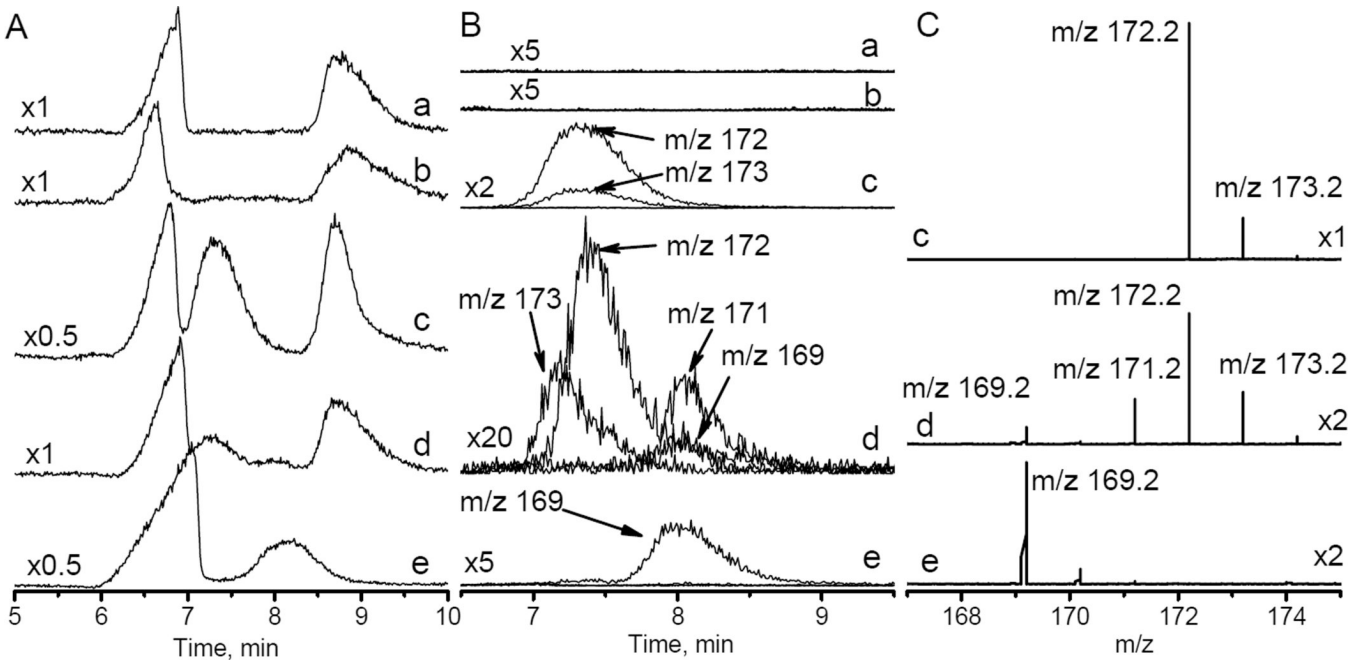

Figure 4.

A. HPLC traces obtained for (a) 20 mM Na-phosphate buffer, pH 7.4; (b) same as (a) + 0.5 mM PF; (c) same as (a) + 1 mM HIMD1; (d) same as (a) + 1 mM HIMD1 + 0.5 mM PF incubated for 1 hour at room temperature; (e) same as (a) + 1 mM HIMD1 + 20 mM PF incubated for 10 hours at room temperature. Numbers on the left indicate the relative scale. **B.** HPLC profiles measured for HIMD1 degradation products with corresponding mass-to-charge ratios (m/z) indicated. Numbers on the left indicate the scale compared to trace (a) in Fig. 4A. Note that asymmetry and small shift of the HPLC peak with m/z=173 for trace (d) compared with trace (c) is presumably due to the presence of hydroxylamine of the HIMD1 in the sample, therefore ionization of both HIMD1 radical and its hydroxylamine may contribute to the HPLC/MS peak with m/z=173. **C.** ESI mass spectra measured for HPLC peaks in region between 7 min and 8.5 min.

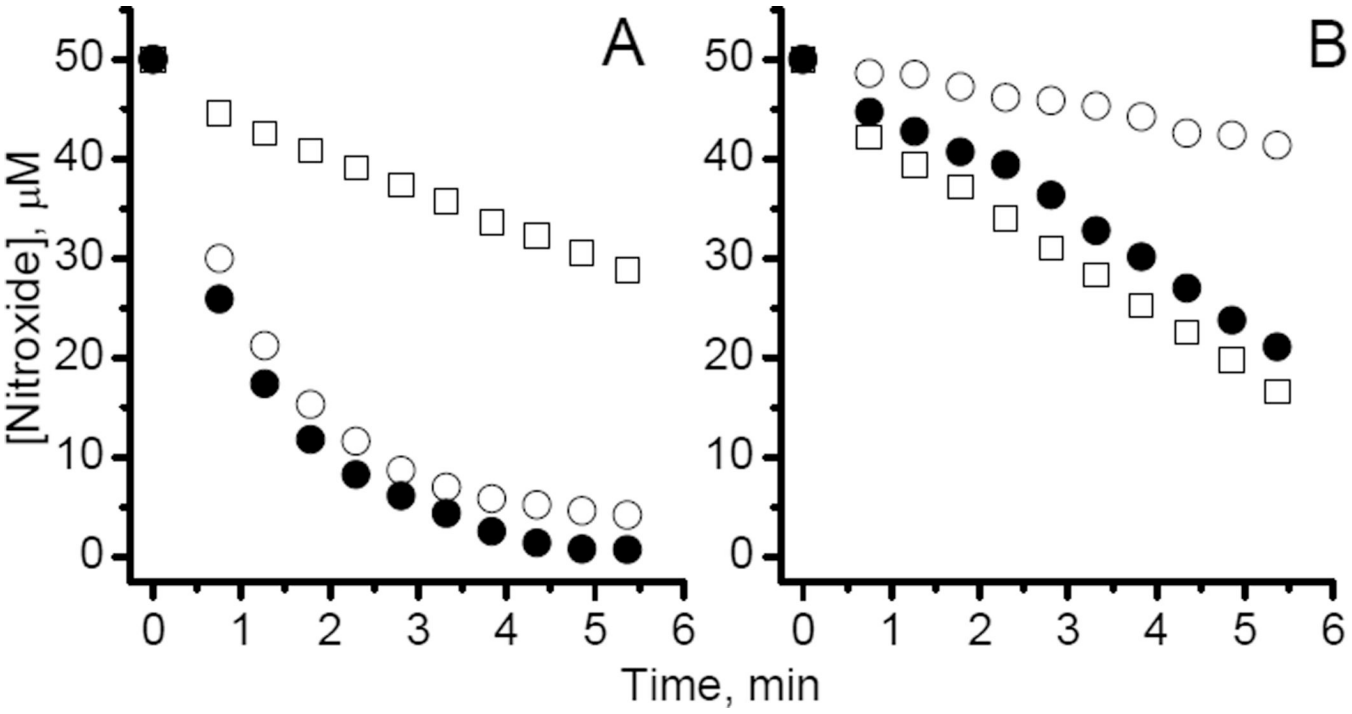

Figure 5.

Kinetics of the EPR signal intensity decay of 50 μM air-saturated aqueous solutions of HIMD1 (A) and HIMD2 (B) in 50 mM phosphate buffer, pH 7.0, at room temperature, in the presence of reducing agent, ascorbate, 10mM (○); radical initiator AIPH, 80 mM (□); and both, 10 mM ascorbate and 80 mM AIPH (●). The rates of the HIMD1 and HIMD2 decay in the presence of AIPH are about of 65 nM/s and 90 nM/s, respectively. The rate of ROO• generation by AIPH was estimated to be close to 90 nM/s (AIPH decomposition rate constant, $k_d \approx 1.2\times10^{-6}$ s^{-1} at 22 °C[53], was approximated from the decomposition rate constants in the temperature range from 40 to 60 °C provided by Waco Pure Chemical Industries, Ltd.; efficiency of the radical escape from the initial radical pair, 0.47[33, 54]).

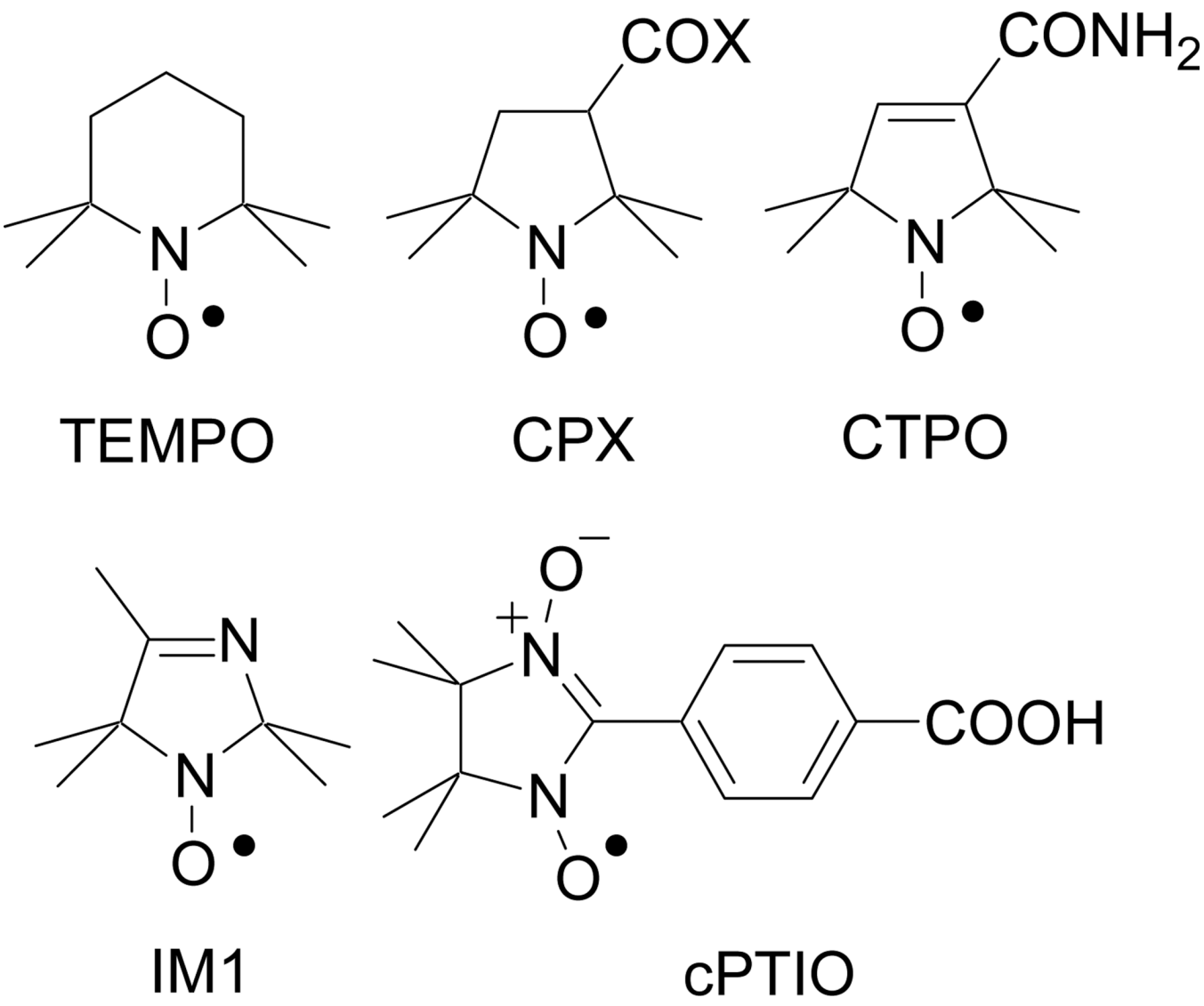

Scheme 1.
Chemical structures of the piperidine nitroxide, TEMPO; pyrrolidine nitroxides, CPX (CP, X=OH, and CMP, X=NH_2); pyrroline nitroxide, CTPO; imidazoline nitroxide, IM1; and nitronyl nitroxide, cPTIO.

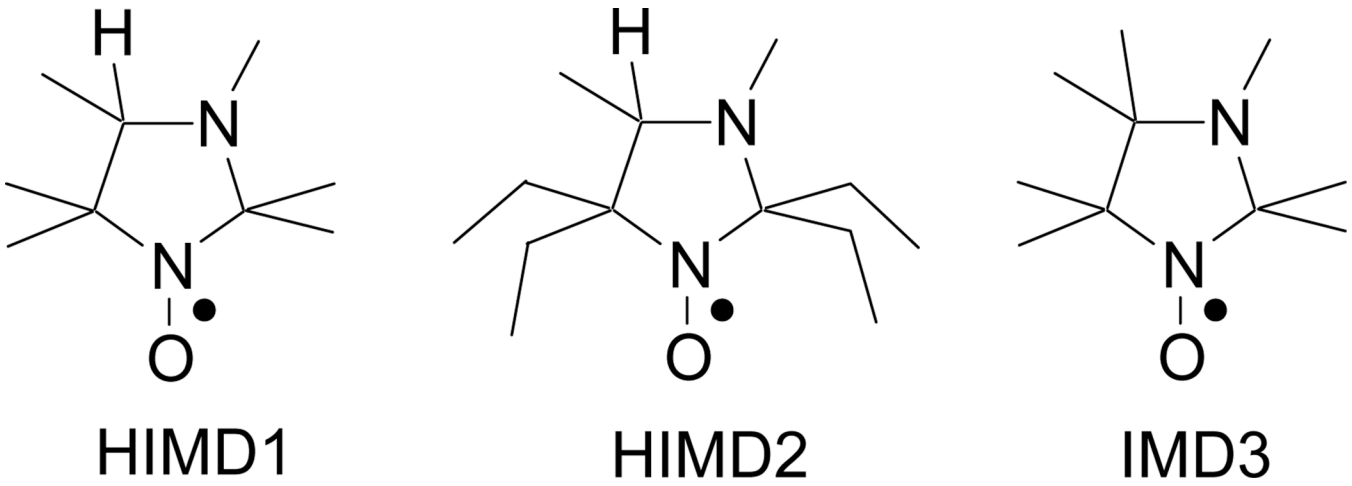

Scheme 2.
Chemical structures of the imidazolidine nitroxides HIMD1, HIMD2 and IMD3.

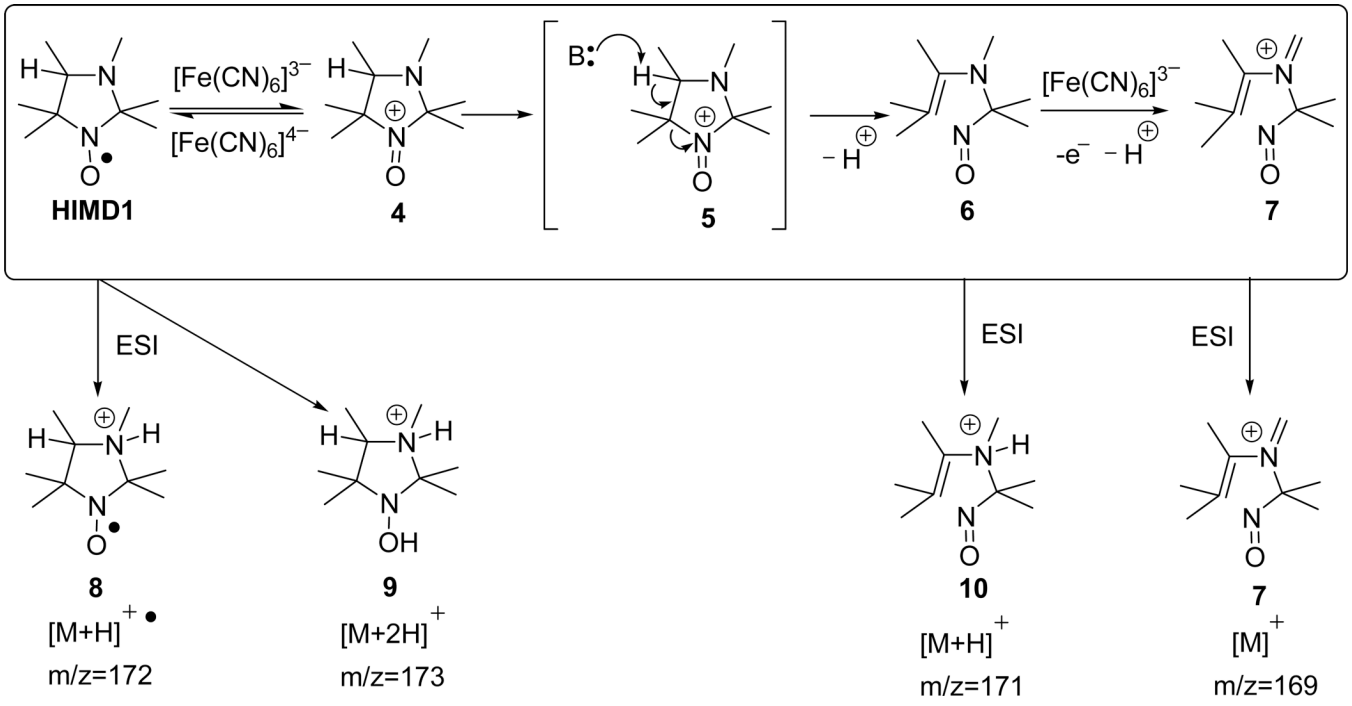

Scheme 3.
A plausible scheme of HIMD1 oxidation by PF (top line). The possible chemical structures of positive ions registered by ESI-MS are shown in the bottom line.

Table 1

Nitroxide oxidation midpoint potentials and bimolecular rate constants (k_{ox}) for the reaction with potassium ferricyanide measured for TEMPO, IM1, HIMD1, HIMD2 and IMD3.

Compound	Midpoint potential, V	k_{ox}, $M^{-1}s^{-1}$
TEMPO	0.67±0.02	stable[b]
IM1	0.95±0.02	stable[b]
HIMD1	0.64[a]	6.3±0.6
HIMD2	0.60[a]	5.8±0.6
IMD3	0.67±0.02	stable[b]

[a] Pseudo midpoint estimation from the value of anodic wave peak potential by subtraction of 0.03 V[52].

[b] Integral EPR spectral intensities of the nitroxides were not affected by the presence of excess of potassium ferricyanide (10 mM) for at least several hours.